

Syntheses, Structure, and Magnetic Behavior of Two New Nickel(II) and Cobalt(II) Dinuclear Complexes with 1,4-Dicarboxylatopyridazine. MO Calculations of the Superexchange Pathway through the Pyridazine Bridge

Albert Escuer,^{*,†} Ramon Vicente,[†] Bouchaid Mernari,[‡] Abdellatif El Gueddi,[‡] and Marcel Pierrot[§]

Departament de Química Inorgànica, Universitat de Barcelona, Diagonal, 647, 08028 Barcelona, Spain, Faculté des Sciences, Université Chouaib Doukkali, B. P. 20, El Jadida, Morocco, and Laboratoire de Bioinorganique Structurale, URA-CNRS 1409, Centre Scientifique St. Jérôme C12, Université d'Aix-Marseille III, 13397 Marseille Cédex 20, France

Received July 23, 1996[⊗]

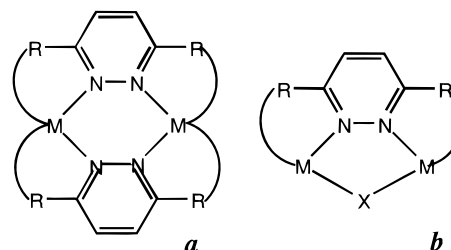
Two new dinuclear complexes of formula $[M_2(dcpz)_2(H_2O)_4]$ in which M is nickel(II) (**1**) or cobalt(II) (**2**) and dcpz is the bridging ligand 1,4-dicarboxylatopyridazine have been synthesized and characterized. The crystal structure for the nickel compound has been solved. Complex **1** crystallizes in the orthorhombic system, space group *Pbca*(61), with $FW = 521.7$, $a = 14.501(3)$ Å, $b = 13.169(3)$ Å, $c = 8.774(2)$ Å, $V = 1675(2)$ Å³, $Z = 4$, and $R = 0.022$. The cobalt compound is isomorphous to **1**. The pyridazine ligand acts as a double bridge between the two paramagnetic centers. Magnetic measurements show moderate antiferromagnetic coupling, with J values of -33.6 cm⁻¹ for **1** and -11.5 cm⁻¹ for **2**. Magnetostructural correlations have been obtained by extended-Hückel MO calculations, and several electronic or structural factors that influence the coupling were analyzed.

Introduction

1,4-Dicarboxylatopyridazine (dcpz) ligand¹ is a potentially tetradentate ligand which can coordinate two metallic centers in a bisbidentate form. Diazine ligands such as pyrazole and 1,2,4-triazole with 3,5 additional coordinating groups or pyridazine and phthalazine with 1,4 coordinating groups can allow two general kinds of dinuclear complexes: one for which the bridges between the metallic ions may be two diazine ligands (M:diazine = 2:2, **a**) or one in which the paramagnetic centers interact through one diazine and one second bridge (M:diazine = 2:1, **b**).

Only a few examples of dinuclear pyrazole, triazole, pyridazine, or phthalazine copper(II),^{2–5} nickel(II),^{6–8} or cobalt(II)^{6–8}

Chart 1



compounds have been structurally and magnetically characterized for the above ligands with a metallic ion/diazine ligand ratio of 2:2. In contrast, a wide number of complexes have been fully characterized for the metallic ion/diazine ligand ratio 2:1, always with a second kind of bridge between the metallic ions, commonly halide or hydroxo.^{9,10} For the later kind of compounds (2:1), which have two different bridges between the paramagnetic centers, successful magnetostructural correlations have been established for X = hydroxo¹¹ or 1,1-azido groups¹² in series of complexes in which the diazine bridge

[†] Universitat de Barcelona.

[‡] Université Chouaib Doukkali.

[§] Université d'Aix-Marseille III.

[⊗] Abstract published in *Advance ACS Abstracts*, April 1, 1997.

- (1) Sueur, S.; Lagrenee, M.; Abraham, F.; Bremard, C. *J. Heterocycl. Chem.* **1987**, *24*, 1285.
- (2) (a) Bayon, J. C.; Esteban, P.; Net, G.; Rasmussen, P. G.; Baker, K. N.; Hahn, C. W.; Gumz, M. M. *Inorg. Chem.* **1991**, *30*, 2572. (b) Ajó, D.; Bencini, A.; Mani, F. *Inorg. Chem.* **1988**, *27*, 2437. (c) Pons, J.; López, X.; Casabó, J.; Teixidor, F.; Caubet, A.; Rius, J.; Miravittles, C. *Inorg. Chim. Acta* **1992**, *195*, 61. (d) Kamiyuki, T.; Okawa, H.; Matsumoto, N.; Kida, S. *J. Chem. Soc., Dalton Trans.* **1990**, 195. (e) Drew, M. G. B.; Yates, P. C.; Esho, F. S.; Trocha-Grimshaw, J.; Lavery, A.; McKillop, K. P.; Nelson, S. M.; Nelson, J. *J. Chem. Soc., Dalton Trans.* **1988**, 2995.
- (3) (a) Slangen, P. M.; van Koningsbruggen, P. J.; Goubitz, K.; Haasnoot, J. G.; Reedijk, J. *Inorg. Chem.* **1994**, *33*, 1121. (b) Koomen-van Oudenniel, W. M. E.; de Graaff, R. A. G.; Haasnoot, J. G.; Prins, R.; Reedijk, J. *Inorg. Chem.* **1989**, *28*, 1128. (c) Prins, R.; Birker, P. J. M. W. L.; Haasnoot, J. G.; Verschoor, G. C.; Reedijk, J. *Inorg. Chem.* **1985**, *24*, 4128. (d) Slangen, P. M.; van Koningsbruggen, P. J.; Haasnoot, J. G.; Jansen, J.; Gorter, S.; Reedijk, J.; Kooijman, H.; Smeets, W. J. J.; Spek, A. L. *Inorg. Chim. Acta* **1993**, *212*, 289. (e) van Koningsbruggen, P. J.; Haasnoot, J. G.; de Graaff, R. A. G.; Reedijk, J.; Slingerland, S. *Acta Crystallogr.* **1992**, *C48*, 1923.
- (4) (a) Mandal, S. K.; Thompson, L. K.; Gabe, E. J.; Charland, J. P.; Lee, F. L. *Inorg. Chem.* **1988**, *27*, 855. (b) Abraham, F.; Lagrenee, M.; Sueur, S.; Mernari, B.; Bremard, C. *J. Chem. Soc., Dalton Trans.* **1991**, 1443.

- (5) Tandon, S. S.; Thompson, L. K.; Hynes, R. C. *Inorg. Chem.* **1992**, *31*, 2210.
- (6) (a) Vreugdenhil, W.; Haasnoot, J. G.; Schoondergang, M. F. J.; Reedijk, J. *Inorg. Chim. Acta* **1987**, *130*, 235. (b) Vos, G.; Haasnoot, J. G.; Verschoor, G. C.; Reedijk, J. *Inorg. Chim. Acta* **1985**, *102*, 187. (c) Groeneveld, L. R.; Le Fèvre, R. A.; de Graaff, R. A. G.; Haasnoot, J. G.; Vos, G.; Reedijk, J. *Inorg. Chim. Acta* **1985**, *102*, 69. (d) Keij, F. S.; de Graaff, R. A. G.; Haasnoot, J. G.; Reedijk, J. *J. Chem. Soc., Dalton Trans.* **1984**, 2093.
- (7) Rosenberg, L.; Thompson, L. K.; Gabe, E. J.; Lee, F. L. *J. Chem. Soc., Dalton Trans.* **1986**, 625.
- (8) (a) Ball, P. W.; Blake, A. B. *J. Chem. Soc., Dalton Trans.* **1974**, 852. (b) Andrew, J. E.; Blake, A. B. *J. Chem. Soc., Dalton Trans.* **1969**, 1408. (c) Ball, P. W.; Blake, A. B. *J. Chem. Soc., Dalton Trans.* **1969**, 1415.
- (9) Chen, L.; Thompson, L. K.; Bridson, J. N. *Inorg. Chem.* **1983**, *32*, 2938 and references therein.
- (10) van Koningsbruggen, P. J.; Gatteschi, D.; de Graaff, R. A. G.; Haasnoot, J. G.; Reedijk, J.; Zanchini, C. *Inorg. Chem.* **1995**, *34*, 5175.
- (11) Thompson, L. K.; Lee, F. L.; Gabe, E. J. *Inorg. Chem.* **1988**, *27*, 39.

shows similar characteristics, whereas the Cu–X–Cu bond angle has a wide range of values.

From the magnetic point of view, it is well-known that the two types of complexes commonly show strong antiferromagnetic superexchange. For the 2:1 compounds, the contribution of the interaction through the superexchange pathway of the diazine ligand to the experimental J value is commonly masked by the interaction through the second bridge, which may also be strongly antiferromagnetic; in contrast, the compounds with only diazine bridging ligands, ratio 2:2, allow the coupling to be studied adequately, focusing our attention exclusively on the diazine superexchange pathway. In this work, we have synthesized two new nickel(II) (**1**) and cobalt(II) (**2**) complexes with the general formula $[M_2(\text{dcpz})_2(\text{H}_2\text{O})_4]$ derived from the 1,4-dicarboxylatopyridazine bridging ligand (dcpz) and we attempt to establish the superexchange mechanism by means of modelization of the dinuclear bis(diazine) bridging complexes, together with the expected magnitude of the J coupling parameter for the copper(II), nickel(II), and cobalt(II) series of analogous compounds. After comparison of the bibliographic data for related compounds, several magnetically relevant factors, such as the ring size, bond angles and R coordinating group were analyzed.

Experimental Section

Synthesis. A solution of 5 mmol of the H_2dcpz ligand was added to an aqueous solution of 5 mmol of nickel(II) chloride hexahydrate. The mixture was gently heated at 40 °C for 1 h and allowed to stand. Slow evaporation of the resulting solution gave blue crystals of **1** after several days. The red analogous compound of cobalt(II) was obtained in the same manner as a microcrystalline product. Anal. Calcd (Found) for $\text{C}_{12}\text{H}_{12}\text{N}_4\text{Ni}_2\text{O}_{12}$: C, 27.63 (26.9); N, 10.74 (10.5); H, 2.32 (2.6). Anal. Calcd (Found) for $\text{C}_{12}\text{H}_{12}\text{N}_4\text{Co}_2\text{O}_{12}$: C, 27.61 (26.5); N, 10.73 (10.4); H, 2.32 (2.6). The IR spectra of the two compounds were virtually identical in the 4000–400 cm^{-1} range. Characteristic $\nu(\text{OH})$ bands appear in the 3300–3500 cm^{-1} region, $\nu(\text{COO})$ appears at 1636 cm^{-1} for **1** and at 1628 cm^{-1} for **2**.

Spectral and Magnetic Measurements. IR spectra were recorded on a Nicolet 520 FTIR spectrophotometer. Magnetic measurements were carried out on polycrystalline samples with a pendulum-type magnetometer (Manics DSM8) equipped with a helium continuous-flow cryostat working in the 4–300 K range under a magnetic field of ~ 1.5 T. Diamagnetic corrections were estimated from Pascal tables.

Crystal Data Collection and Refinement. A prismatic blue crystal of **1** ($0.12 \times 0.12 \times 0.20$ mm) was selected and mounted on an Enraf-Nonius CAD4 diffractometer. Intensities were collected with graphite-monochromatized Mo $K\alpha$ radiation using the $\omega/2\theta$ technique, (2791 reflections collected, 1308 assumed as independent). Selected reflections were measured every 2 h as orientation and intensity control; significant decay was not observed. The crystallographic data, conditions retained for the intensity data collection and some features of the structure refinement, are listed in Table 1. The program used to solve the structure was MULTAN11/82,¹³ completed by Fourier synthesis. Hydrogen atoms linked to C(4) and C(5) were introduced into idealized positions in the calculations but were not refined. Hydrogen atoms of the water molecules were unambiguously located on the Fourier difference and introduced into the calculations before the last refinement cycles. Molecular graphics: ORTEPII and PLUTON.¹⁴ The number

Table 1. Crystal Data for $[\text{Ni}_2(\text{dcpz})_2(\text{H}_2\text{O})_4]$ (**1**)

chem formula	$[\text{C}_{12}\text{H}_{12}\text{N}_4\text{Ni}_2\text{O}_{12}]$
a , Å	14.501(3)
b , Å	13.169(3)
c , Å	8.774(2)
V , Å ³	1675(2)
Z	4
formula weight	521.7
space group	$Pbca(61)$
T , °C	20
$\lambda(\text{Mo } K\alpha)$, Å	0.710 69
d_{calc} , $\text{g}\cdot\text{cm}^{-3}$	2.068
$(\text{Mo } K\alpha)$, cm^{-1}	23.3
R^a	0.022
wR^b	0.028

$$^a R = \sum(|F_o| - |F_c|)/\sum|F_o|. \quad ^b wR = [\sum w(|F_o| - |F_c|)^2/\sum w|F_o|^2]^{1/2}.$$

Table 2. Fractional Atomic Coordinates for $[\text{Ni}_2(\text{dcpz})_2(\text{H}_2\text{O})_4]$ (**1**) and Their Standard Deviations

atom	x/a	y/b	z/c	B , Å ²
Ni	0.06725(2)	0.10530(3)	0.60077(4)	1.069(7)
OW(1)	0.1213(2)	0.1460(2)	0.3885(3)	1.78(5)
OW(2)	0.5145(2)	0.4426(2)	0.1901(3)	1.92(5)
O(1)	−0.1959(1)	−0.1110(2)	0.3101(3)	1.63(4)
O(2)	−0.3244(2)	−0.0216(2)	0.2785(3)	2.05(5)
O(3)	0.0357(1)	0.2517(2)	0.6536(3)	1.66(4)
O(4)	−0.0785(2)	0.3657(2)	0.6402(3)	2.31(5)
N(1)	−0.1132(2)	0.0404(2)	0.4466(3)	1.01(5)
N(2)	−0.0655(2)	0.1142(2)	0.5153(3)	1.14(5)
C(3)	−0.1059(2)	0.2033(2)	0.5425(4)	1.26(6)
C(4)	−0.1978(2)	0.2218(2)	0.5084(4)	1.80(7)
C(5)	−0.2469(2)	0.1455(3)	0.4401(4)	1.88(6)
C(6)	−0.2010(2)	0.0562(2)	0.4077(4)	1.35(6)
C(7)	−0.2446(2)	−0.0332(2)	0.3250(4)	1.40(6)
C(8)	−0.0445(2)	0.2813(2)	0.6188(4)	1.42(6)

of refined parameters was 136. Largest difference peak and hole 0.36/−0.42 $\text{e}\cdot\text{Å}^{-3}$, Maximum shift/error 0.01. Atomic coordinates are given in Table 2.

Results and Discussion

Description of the Structure. X-ray structure of $[\text{Ni}_2(\text{dcpz})_2(\text{H}_2\text{O})_4]$ (1**).** The structure consists of $[\text{Ni}_2(\text{dcpz})_2(\text{H}_2\text{O})_4]$ isolated centrosymmetric dimeric units (Figure 1). Relevant bond lengths and angles are gathered in Table 3. The molecule consists of two nickel(II) ions in octahedral environment bridged by two pyridazine ligands. Each nickel ion is coordinated to two nitrogen atoms, two oxygen atoms (carboxylate), and two water molecules in axial position. The two O–Ni–N bond angles in the equatorial plane are close to 79.5°, whereas N(1)′–Ni–N(2) and O(1)′–Ni–O(3) are 106.2(1) and 94.80(9)°, respectively. The two pyridazine rings and the two nickel atoms lie in the same plane, as commonly occurs in this kind of dinuclear system. Relevant data useful for the magnetic correlations were those related to the bridging fragment of the molecule. Bond lengths and angles compare well with previously reported data for similar complexes (Table 4): bond lengths Ni–N(1)′ 2.073(2) Å and Ni–N(2) 2.069(2) Å are slightly shorter than those reported for other Ni_2 –pyridazine₂ systems such as $[\text{Ni}_2(\text{ppd})_2(\text{H}_2\text{O})_4]^{4+}$ and close to the values for $[\text{Ni}_2(\text{dph})_2(\text{H}_2\text{O})_4]^{4+}$; bond angles Ni–N(2)–N(1) 127.1(1) and Ni–N(1)′–N(2)′ 126.7(1)° are close to those reported for the above compounds and the Ni⋯Ni distance 3.824(1) Å is intermediate between the 3.920(1) and the 3.791(4) Å reported for the ppd and dph compounds, respectively. Major differences were found when they were compared with the $[\text{Ni}_2(\text{abpt})_2\text{Cl}_2(\text{H}_2\text{O})_2]^{2+}$ complex for which Ni–N = 2.013(1) and 2.029(1) Å, Ni–N–N = 132.63(8) and 134.22(8)°, and the Ni⋯Ni distance is 4.135(3) Å.

(12) Thompson, L. K.; Tandon, S. S.; Manuel, M. E. *Inorg. Chem.* **1995**, *34*, 2356.

(13) Main, P.; Fiske, S. J.; Hull, S. E.; Lessinger, L.; Germain, G.; Declercq, J. P.; Woolfson, M. M. MULTAN 11/82: a system of computer programs for the automatic solution of crystal structures from X-Ray diffraction data. University of York (England) and Lovain (Belgium), 1982.

(14) Johnson, C. K. ORTEPII, Report ORNL-5138; Oak Ridge National Laboratory, Oak Ridge, TN, 1976. Spek, A. L. PLUTON-92, University of Utrecht, 3584, CH Utrecht, The Netherlands, 1992.

(15) Wall, P. W.; Blake, A. B. *J. Chem. Soc., Dalton Trans.* **1974**, 852.

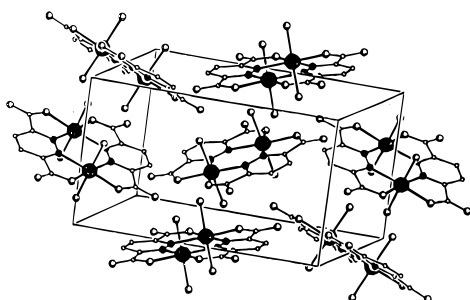
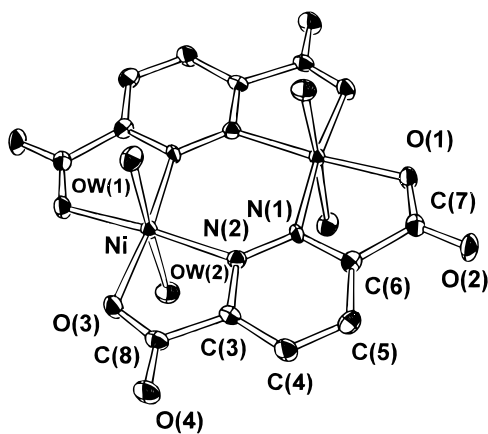


Figure 1. ORTEP atom labeled scheme for $[\text{Ni}_2(\text{dcpz})_2(\text{H}_2\text{O})_4]$ (**1**) and a view of the unit cell.

Table 3. Selected Bond Distances (Å) and Angles (deg) for $[\text{Ni}_2(\text{dcpz})_2(\text{H}_2\text{O})_4]$ (**1**)

Nickel Environment			
Ni–OW(1)	2.091(2)	Ni–O(3)	2.034(2)
Ni–OW(2)	2.086(2)	Ni–N(1)′	2.073(2)
Ni–O(1)′	2.025(2)	Ni–N(2)	2.069(2)
dcpz Ligand			
C(7)–O(1)	1.252(4)	C(3)–C(4)	1.388(5)
C(7)–O(2)	1.235(4)	C(4)–C(5)	1.370(5)
C(8)–O(3)	1.264(4)	C(5)–C(6)	1.381(5)
C(8)–O(4)	1.231(4)	C(3)–C(8)	1.514(4)
N(1)–N(2)	1.337(3)	C(6)–C(7)	1.521(4)
N(1)–C(6)	1.334(4)		
N(2)–C(3)	1.333(4)		
Nickel Environment			
OW(1)–Ni–OW(2)	177.22(9)	OW(2)–Ni–N(2)	89.70(9)
OW(1)–Ni–O(1)′	89.38(9)	O(1)′–Ni–O(3)	94.80(9)
OW(1)–Ni–O(3)	92.55(9)	O(1)′–Ni–N(1)′	79.37(9)
OW(1)–Ni–N(1)′	86.44(9)	O(1)′–Ni–N(2)	174.42(9)
OW(1)–Ni–N(2)	90.62(9)	O(3)–Ni–N(1)′	174.09(9)
OW(2)–Ni–O(1)′	90.56(9)	O(3)–Ni–N(2)	79.62(9)
OW(2)–Ni–O(3)	90.22(9)	N(1)′–Ni–N(2)	106.2(1)
OW(2)–Ni–N(1)′	90.82(9)	Ni–N(1)′–N(2)′	126.7(1)
		Ni–N(2)–N(1)	127.1(1)
dcpz Ligand			
N(1)–N(2)–C(3)	119.6(6)	C(4)–C(5)–C(6)	117.7(3)
N(2)–N(1)–C(6)	119.7(2)	N(1)–C(6)–C(5)	122.7(3)
N(2)–C(3)–C(4)	122.5(3)	N(1)–C(6)–C(7)	113.5(3)
N(2)–C(3)–C(8)	114.7(3)	C(5)–C(6)–C(7)	123.8(3)
C(4)–C(3)–C(8)	122.7(3)	O(1)–C(7)–O(2)	126.5(3)
C(3)–C(4)–C(5)	117.7(3)	O(3)–C(8)–O(4)	127.6(3)

Magnetic Properties. The plots of χ_M per dimeric unit vs T of **1** and **2** are shown in Figure 2. The shape of the plots agrees with antiferromagnetic $[\text{NiNi}]$ and $[\text{CoCo}]$ entities: the χ_M plots show maximum susceptibility at 51 K for **1** and at 25 K for **2**, whereas the $\chi_M \cdot T$ values decrease continuously from room temperature ($\chi_M \cdot T$ values 2.32 and 4.95 $\text{cm}^3 \cdot \text{K} \cdot \text{mol}^{-1}$, respectively) and tend to zero at low temperatures.

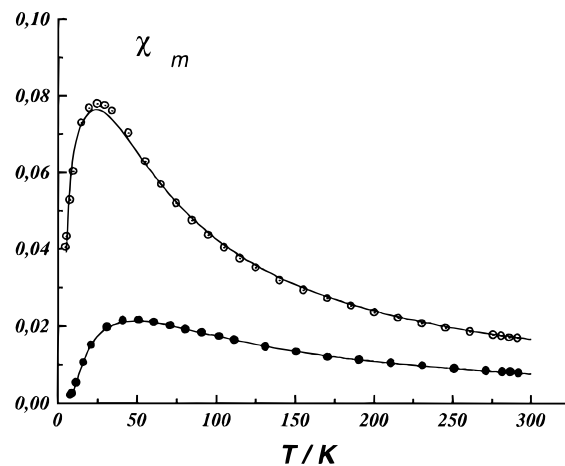


Figure 2. Experimental and calculated χ_M ($\text{cm}^3 \cdot \text{mol}^{-1}$) vs T for $[\text{Ni}_2(\text{dcpz})_2(\text{H}_2\text{O})_4]$ (●) and $[\text{Co}_2(\text{dcpz})_2(\text{H}_2\text{O})_4]$ (○). Solid lines show the best fit indicated in the text.

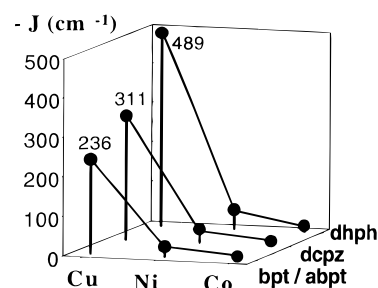


Figure 3. Plot of the experimental superexchange parameter J for several Cu, Ni, and Co(II) complexes for three series of diazine ligands.

Fit of the experimental data was performed to isotropic expressions derived from the Hamiltonian $H = -JS_1S_2$ for $[\text{NiNi}]$ or $[\text{CoCo}]$ pairs $\chi_M = N\beta^2 g^2 / kT \cdot f(J, T)$ where $f(J, T)$ is

$$(2 \exp(J/kT) + 10 \exp(3J/kT)) / (1 + 3 \exp(J/kT) + 5 \exp(3J/kT))$$

or

$$(2 \exp(J/kT) + 10 \exp(3J/kT) + 28 \exp(6J/kT)) / (1 + 3 \exp(J/kT) + 5 \exp(3J/kT) + 7 \exp(6J/kT))$$

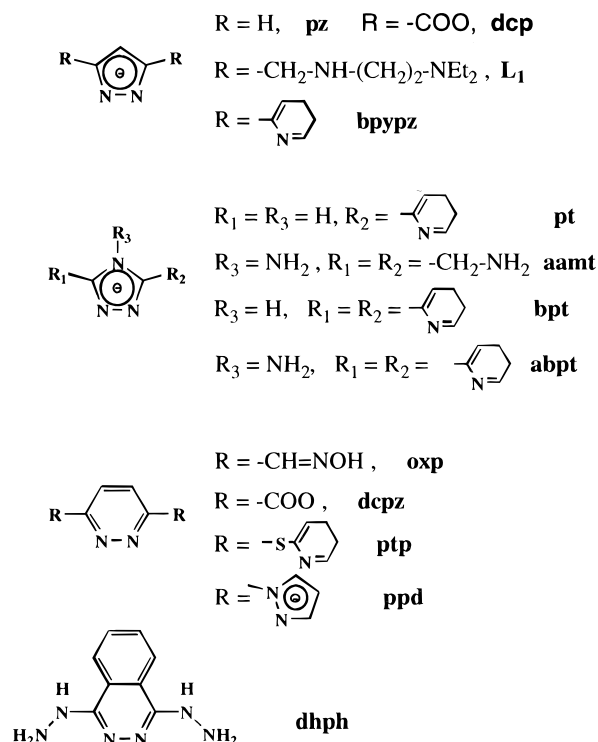
for a $[\text{NiNi}]$ or $[\text{CoCo}]$ pair, respectively, by minimizing the function $R = \sum (\chi_M^{\text{calcd}} - \chi_M^{\text{obs}})^2 / \sum (\chi_M^{\text{obs}})^2$. The best-fit parameters were $J = -33.6(2) \text{ cm}^{-1}$, $g = 2.287(5)$, $R = 1.4 \times 10^{-4}$ for **1** and $J = -11.5(3) \text{ cm}^{-1}$, $g = 2.40(2)$, $R = 1.1 \times 10^{-3}$ for **2**.

Magnetic Properties of the Diazine Bridges. In order to compare bibliographic results, all the reported J values correspond to those calculated using the Hamiltonian $H = -JS_1S_2$ for the cases $S = 1/2$, 1, and $3/2$. The J coupling constants for **1** and **2** are of the same range of magnitude as those found for similar nickel or cobalt(II) complexes (Table 4). If these data are compared with the J values reported for the analogous copper dinuclear compounds $[\text{Cu}_2(\text{bpt})_2(\text{CF}_3\text{SO}_3)(\text{H}_2\text{O})]^{2+}$ ($J = -236 \text{ cm}^{-1}$),^{3c} $[\text{Cu}_2(\text{dcpz})_2(\text{H}_2\text{O})_2]^{4+}$ ($J = -311 \text{ cm}^{-1}$)¹⁶ and $[\text{Cu}_2(\text{dhph})_2(\text{H}_2\text{O})_2(\text{ClO}_4)_2]^{2+}$ ($J = -489 \text{ cm}^{-1}$),⁵ some interesting experimental data can be extracted from Figure 3: the J value for the triazole bridged dimers is always lower than for the six-membered diazine rings, as is generally accepted; the magnitude of the coupling constants follows in the three cases the order

(16) Mernari, B. Ph.D. Thesis, Université Mohammed V, Rabat, Morocco, 1991.

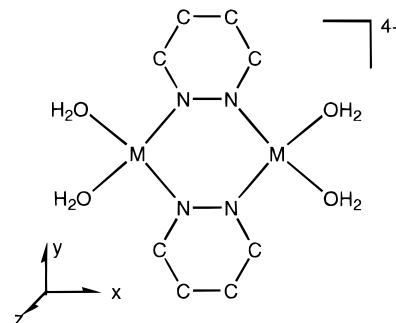
Table 4. Structural and Magnetic Significant Parameters for the Characterized Dinuclear Nickel Compounds with Double Diazine Bridge

compound	M–N, Å	M–N–N, deg	N–M–N, deg	<i>J</i> , cm ⁻¹	ref
[Ni ₂ (abpt) ₂ Cl ₂ (H ₂ O) ₂]Cl ₂	2.013 2.029	132.6 134.2	93.0	-25.0	6d
[Ni ₂ (dhph) ₂ (H ₂ O) ₄]Cl ₄	2.072 2.080	125.6 124.8	109.6	-46.9	8
[Ni ₂ (dcpz) ₂ (H ₂ O) ₄]	2.069 2.073	127.1 126.7		-33.6	<i>a</i>
[Ni ₂ (ppd) ₂ (H ₂ O) ₄]Cl ₄	2.121 2.130	127.3 126.9	105.8	-29.6	7
[Co ₂ (abpt) ₂ Cl ₂ (H ₂ O) ₂]Cl ₂	isomorphous to the Ni compd			-8.0	6d
[Co ₂ (dhph) ₂ (H ₂ O) ₄]Cl ₄	isomorphous to the Ni compd			-14.7	15
[Co ₂ (dcpz) ₂ (H ₂ O) ₄]	isomorphous to the Ni compd			-11.5	<i>a</i>

^a This work.**Chart 2**

$J_{[\text{CuCu}]} \gg \gg J_{[\text{NiNi}]} > J_{[\text{CoCo}]}$. Finally, the *J* values for the dhph complexes are roughly 50% greater than those found for the dcpz compounds despite the minimal differences in the bond parameters in the bridging region.

The first step to try to correlate the above magnetic results was the detailed analysis of the correlations previously reported by other authors, (not always in accordance!) for these ligands: (a) It is commonly accepted that pyridazines and phthalazines allow greater coupling than pyrazole or triazole ligands. (b) Bencini^{2d} et al. pointed out, from experimental data and MO calculations on the [Cu₂(H₂bpz)₂(μ-pz)₂(μ-Cl)]⁻ compound, that the dihedral angle of 92° between the bridging pyrazole groups does not drastically reduce the coupling between the copper ions, in basis on a σ superexchange pathway. This result was confirmed by two new nonplanar compounds with μ-pyrazole^{2b,d} and μ-pyridazine^{4a} which show very strong coupling despite their distortion from planarity. (c) the M₂-μ-diazine₂ compounds generally show four M–N–N bond angles close to 135° for the pyrazole and triazole bridges, whereas the M–N–N bond angles are close to 125° for the six-membered diazines. Reedijk et al. correlated the low *J* values found for the copper compounds bridged by the asymmetric pt ligand to the Cu–N–N bond angles close to the 125–140° found in a series of four compounds.^{3a,d} (d) The π superexchange pathway was in

Chart 3

most cases assumed as relevant in the coupling, whereas other authors related the *J* parameter exclusively to a σ pathway between the paramagnetic centers and the MOs of the bridging ligands.

MO Calculations and Magnetostructural Correlations. In order to approach the superexchange pathway for the pyridazine bridged compounds, MO extended-Hückel calculations were performed by means of the CACAO program¹⁷ on a dimeric unit that models the reported dinuclear systems with double diazine bridge under *D*_{2h} symmetry.

Calculations were performed for M = Cu, Ni, and Co(II). Bond lengths used were M–N and M–O 2.0 Å for M = Cu, 2.1 Å for M = Ni or Co, and C–C, C–N, and N–N 1.36 Å, bond angles were 120 and 108° for the pyridazine and the five-membered rings, respectively, whereas the M–N–N and N–M–N bond angles were used as variable parameters throughout the different calculations. For M = Ni and Co, octahedral coordination was achieved adding two water molecules by metallic ion along the *z* axis, at the same M–OH₂ 2.1 Å distance. The used computational parameters were the standard of the CACAO program. To correlate the results of the calculations to the experimental *J* values, we used the relationship between the square of the gaps between the pairs of MO of the same symmetry (named ΣΔ²) and the antiferromagnetic component of *J* pointed out by Hoffmann,¹⁸ which assumes that the ferromagnetic component of *J* and the exchange Coulomb integrals remain almost constant for series of similar complexes. The MO diagram for M = Ni and pyridazine bridge, calculated from the M–N–N and N–M–N values of 127.5° and 105°, respectively, is shown in Figure 4. As would be expected, the main contribution to *J*_{AF} is due to the gap between the symmetric and antisymmetric combination of the magnetically active d_{xy} orbitals of the nickel atoms with the adequate MOs of the pyridazine bridges, as schematized in

(17) Mealli, C.; Proserpio, D. M. CACAO program (Computed Aided Composition of Atomic Orbitals). *J. Chem. Educ.* **1990**, *67*, 399.

(18) Hay, P. J.; Thibault, J. C.; Hoffmann, R. *J. Am. Chem. Soc.* **1975**, *97*, 4884.

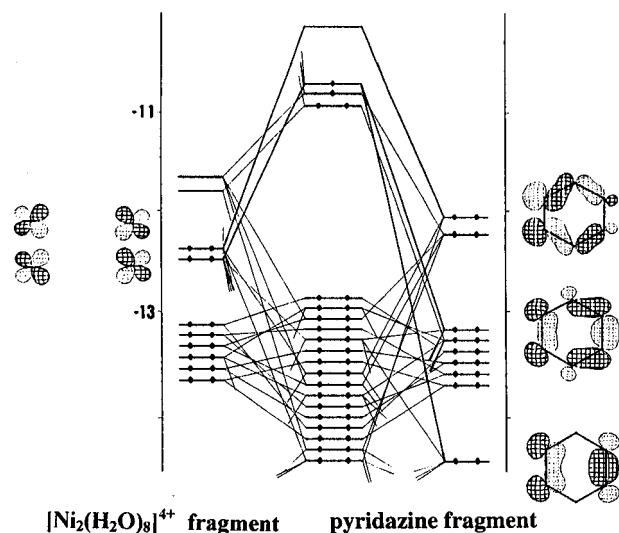


Figure 4. MO diagram for the $[\text{Ni}_2(\text{pyridazine})_2(\text{H}_2\text{O})_8]^{4+}$ modelization of $[\text{Ni}_2(\text{dcpz})_2(\text{H}_2\text{O})_4]$. Significant contributions of the two $[\text{Ni}_2(\text{H}_2\text{O})_8]^{4+}$ and $[(\text{pyridazine})_2]$ fragments are schematized in the figure.

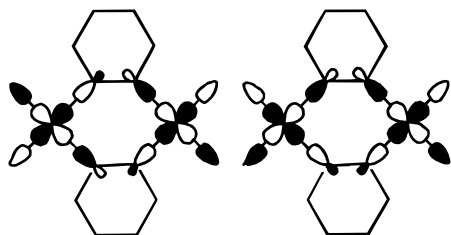


Figure 5. Scheme of the two MOs obtained from the $d_{xy} + d_{xy}$ and $d_{xy} - d_{xy}$ combinations of the magnetically active atomic orbitals of the nickel fragments with the adequate MO of the pyridazine. The gap between these two MOs, with strict σ interaction pathway, is the main contribution to the antiferromagnetic component of J for $[\text{M}_2(\text{dcpz})_2(\text{H}_2\text{O})_4]$ system.

Figure 5. The great difference in energy between the b_{1g} and the b_{2u} MO combinations of the pyridazine ligands produces the large gap between the two MOs with d_{xy} participation. The MOs that have some contribution from the d_{z^2} active orbitals of the nickel ions, b_{3u} and a_g , show a smaller gap (less than a 10% of the xy gap), as would be expected by taking into account the smaller overlap with the MOs of the bridge. For $M = \text{copper}$ ion, the xy gap is similar to the case of nickel and for $M = \text{cobalt}$, similar values were also found together with an almost negligible contribution from the d_{xz} MO pair.

For the three studied cases, the most immediate result obtained from these calculations was that the contribution of the MOs with π symmetry was zero, even in the case of the cobalt ion, for which there is one magnetically active t_{2g} atomic orbital. The above results allow a σ superexchange pathway to be assigned.

Calculations performed for $M = \text{Cu, Ni, and Co}$ for the triazole bridging ligands ring, taking the $M-N-N$ and $N-M-N$ bond angles as 135 and 90° , respectively, show as their most relevant feature a lower $\Sigma\Delta^2$ for all of them, as is experimentally found from magnetic data analysis. For this ligand, the superexchange pathway is also shown to be exclusively σ for $M = \text{Cu and Ni}$ but some nonnegligible interaction was found in the case of $M = \text{Co}$, probably due to the higher π electronic density in the five-membered ring.

Finally, calculations performed for the two bridging ligands, varying the bond angles in the M_2N_4 fragment, show that the antiferromagnetic component of J reaches its maximum for the parameters $M-N-N = 135^\circ$, $N-M-N = 90^\circ$ and decreases

Table 5. Structural and Magnetic Significant Parameters for the Characterized Dinuclear Copper Compounds with Double Diazine Bridge

compound	M-N, Å	M-N-N, deg	N-M-N, deg	J , cm^{-1}	ref
$[\text{Cu}_2(\text{L1})_2]$	1.929	131.0		-428	2d
$[\text{Cu}_2(\text{bypyz})_2(\text{H}_2\text{O})_2]$	1.954	130.6		-362	2c
$[\text{Cu}_2(\text{dcp})_2]$	1.942	134.0	91.7	-200	2a
$[\text{Cu}_2(\text{btp})_2(\text{CF}_3\text{SO}_3)(\text{H}_2\text{O})]$	1.911	133.8		-236	3c
	1.907	133.9	90.2		
	1.942	135.2	90.1		
	1.936	134.9			
		134.8			
		134.5			
$[\text{Cu}_2(\text{aamt})_2(\text{Br})(\text{H}_2\text{O})]$	1.950	134.2	92.1	-220	3b
	1.937	133.7			
$[\text{Cu}_2(\text{abpt})_2(\text{H}_2\text{O})_4]$	1.954	135.1	91.9	-193	3e
	1.960	132.9			
$[\text{Cu}_2(\text{oxp})_2(\text{ClO}_4)_2(\text{H}_2\text{O})_2]$	2.027	127.3	105.5	-536	4b
	2.014	126.8			
$[\text{Cu}_2(\text{ptp})_2(\text{Cl})](\text{ClO}_4)_3]$	2.002	118.6	85.4	-479	4a
	2.018	85.8			
$[\text{Cu}_2(\text{dcpz})_2(\text{H}_2\text{O})_4]$	2.008	127.5	104.5	-311	16
	2.012	127.9			
$[\text{Cu}_2(\text{dhph})_2(\text{H}_2\text{O})_2(\text{ClO}_4)_2]^{2+}$	1.981	127.4	107.3	-489	
	1.996	124.8			

when the $N-M-N$ bond angle increases as a consequence of the smaller overlap for large angles. This result is in good accordance with the correlation proposed by Reedijk for asymmetric diazine bridges.^{3d}

The above results as a function of the structural parameters in the bridging region gave the general trends of the coupling pathway but do not explain that in series of copper dinuclear compounds showing fully comparable bond parameters in the Cu_2N_4 inner ring has extreme variations of the J coupling parameter. This evidences that factors other than the bond parameters in the bridging region should be taken into account to the complete explanation of the J values. Analyzing Table 5, a new factor may be added: the R substituents of the diazine ring affect drastically the J values. These substituents may indirectly influence the electronic density in the bridging region in two different ways: either they activate or deactivate the aromatic ring or the electronegativity of the group linked to the equatorial coordination sites of the paramagnetic ion may tune the J value.¹⁸ It is significant that the lower J coupling values found for the pyrazole and pyridazine series (-200 and -311 cm^{-1} , respectively) are shown by the dcp or dcpz ligands in which the carboxylate group R reduces electronic density, both in the ring and directly on the metallic ion, by means of the four oxygen atoms coordinated in equatorial sites, whereas the L₁ ligand in which R is the strongly basic $\text{CH}_2\text{NH}(\text{CH}_2)_2\text{-NEt}_2$ shows a J value of -428 cm^{-1} , even greater than other J parameters reported for pyridazine bridges.

Another interesting point is that the $J_{[\text{CuCu}]} \gg J_{[\text{NiNi}]} > J_{[\text{CoCo}]}$ relationship indicates that the superexchange is much more effective for the copper systems. When comparing the J values for the diazine copper, nickel, and cobalt derivatives, and taking into account the $n^2|J|$ relation in which n is the number of unpaired electrons for a dimeric unit, we see that $J_{[\text{CuCu}]} \gg 4J_{[\text{NiNi}]} \gg 9J_{[\text{CoCo}]}$ in contrast to the similar $\Sigma\Delta^2$ found for the three ions in the above calculations. Several reasons contribute to the higher efficiency of the superexchange for the copper derivatives: the Cu-N bond distances are generally shorter than the Ni-N bond lengths, which increases the antibonding overlap and produces a great xy antiferromagnetic contribution. On the other hand, the ferromagnetic contributions may be neglected for the copper system, but they should be taken into account for the nickel or cobalt compounds. $J_{[\text{CuCu}]}$, $J_{[\text{NiNi}]}$, and $J_{[\text{CoCo}]}$ for the dcpz compounds may be taken to be

$$J_{|\text{Cu-Cu}|} = J_{xy-xy} = 311 \text{ cm}^{-1}$$

$$J_{|\text{Ni-Ni}|} = 1/4(J_{xy-xy} + J_{z-z}^2 + 2J_{xy-z}^2) = 33.6 \text{ cm}^{-1}$$

$$J_{|\text{CoCo}|} = 1/9(J_{xy-xy} + J_{z-z}^2 + 2J_{xy-z}^2 + 2J_{yz-yz} + 2J_{xy-xz} + 2J_{xz-z}^2) = 11.5 \text{ cm}^{-1}$$

J_{xy-xy} , J_{z-z}^2 , and J_{yz-yz} are the antiferromagnetic contributions to the superexchange, whereas the remaining terms are ferromagnetic contributions. Assuming a σ superexchange pathway, the only important antiferromagnetic contribution should be J_{xy-xy} , and consequently, the J value may be high for copper compounds whereas the ferromagnetic contributions drastically reduce the observed J value for the nickel and cobalt dinuclear systems. From these experimental data, the $J_{|\text{CuCu}|} = 10J_{|\text{NiNi}|} = 30J_{|\text{CoCo}|}$ ratio of J values is reasonable for this kind of compound. This is not surprising, and the literature offers examples of similar behavior such as the widely studied μ -oxalato system,¹⁹ for which the μ -oxalato copper dinuclear compounds show J values close to -300 cm^{-1} whereas the μ -oxalato nickel dinuclear compounds show J values always close to -30 cm^{-1} , or the less studied μ -carbonato system, even diamagnetic for copper dinuclear compounds²⁰ ($-J > 1000 \text{ cm}^{-1}$) whereas the J parameter is close to -100 cm^{-1} for nickel(II) complexes.²¹

(19) Bataglia, L. P.; Bianchi, A.; Bonamartini-Corradini, A.; Garcia-España, E.; Micheloni, M.; Julve, M. *Inorg. Chem.* **1988**, *27*, 4147.

(20) Sletten, J.; Hope, H.; Julve, M.; Kahn, O.; Verdager, M.; Dworkin, A. *Inorg. Chem.* **1988**, *27*, 542.

Conclusions

Two new pyridazine double-bridged complexes of formula $[\text{M}_2(\text{dcpz})_2(\text{H}_2\text{O})_4]$ in which M is nickel(II) (**1**) or cobalt(II) (**2**) and dcpz is the bridging ligand 1,4-dicarboxylatopyridazine have been structurally characterized and their magnetic properties have been correlated in several ways by comparison with the structural and magnetic properties of series of related compounds. Experimental results together with MO calculations suggest that the J coupling parameter may be tuned mainly by adequate choice of the diazine ring (J for six-membered rings $> J$ for five membered-rings), but taking into account that the above correlation may be reversed changing the coordinating R pendant arms. M–N–N bond angles also diminish the coupling for the two kind of rings (greater bond angles, lower coupling). For the same diazine ring and R, and taking the metallic ion as a variable parameter, the ratio $J_{|\text{CuCu}|} = 10J_{|\text{NiNi}|} = 30J_{|\text{CoCo}|}$ was found for three different series of ligands.

Acknowledgment. This work was financially supported by the CICYT PB93/0772.

Supporting Information Available: Tables giving a structure determination summary, atomic positional coordinates, complete bond lengths and angles, H atom coordinates, anisotropic displacement parameters, and crystallographic details for $[\text{Ni}_2(\text{dcpz})_2(\text{H}_2\text{O})_4]$ (6 pages). Ordering information is given on any current masthead page.

IC9608859

(21) Escuer, A.; Vicente, R.; Kumar, S. B.; Solans, X.; Font-Bardia, M.; Caneschi, A. *Inorg. Chem.* **1996**, *35*, 3094.